hep-lat/9503011 BI-TP 95/12

# DECONFINEMENT AND HOT HADRONS IN CRAYS AND QUADRICS <sup>a</sup>

G. BOYD

Fakultät für Physik, Universität Bielefeld Postfach 100131, D-33501 Bielefeld, Germany

### Abstract

The equation of state of pure QCD, obtained from lattice QCD, is discussed for temperatures ranging from  $0.9T_{\rm c}$  to  $4T_{\rm c}$ , as well as results on screening masses, the chiral condensate, and the pion decay constant close to the deconfinement phase transition in the confined phase of QCD. The equation of state differs significantly from that of a free gas. There is little evidence of a temperature dependence in the chiral condensate or the meson properties, but perhaps some for the nucleon screening mass. Above the phase transition one sees non-perturbative effects, even though hadron correlators show the existence of deconfined quarks.

## 1 Introduction

The study of hadronic matter at high temperature and / or density is receiving increasing attention, both experimentally and theoretically. It is important to gain a good understanding of the predictions of QCD in this regime as soon as possible. There are many approaches to this task, some of which are presented elsewhere in these proceedings. Each is advantageous for some aspect of the problem. One needs to combine them all to understand what QCD predicts over the entire range of temperatures and densities relevant for heavy ion collisions.

Recent results from one of the major theoretical players, the lattice regulation of QCD at finite temperature, will be presented below. An introduction to lattice QCD may be found, for example, in [1, 2].

When one is close to the phase transition, many of the traditional approaches to QCD run into problems, as both low temperature and high temperature expansions need to be extrapolated into regions far from the regions in which they are known to be secure. The lattice may well be the only satisfactory approach in this region.

The equation of state, both for nuclear matter just below the deconfinement transition, and for the quark-gluon plasma above the phase transition, is required information for, amongst others, hydrodynamic models attempting to describe the

<sup>&</sup>lt;sup>a</sup> Summary of invited talks presented at the Hirschegg Workshop XXIII 'Dynamical Properties of Hadrons in Nuclear Matter', Jan. 16–21, Hirschegg, Austria and 'Chiral Dynamics in Hadrons and Nuclei', Feb. 6–10, Seoul, Korea

evolution of the quark gluon plasma. Since the couplings and masses are not small below  $2T_c$  the lattice approach is the obvious method to use.

Despite extensive studies of the QCD phase transition [2, 3] little is known with certainty about the changes in the excitation spectrum. In particular, the properties of the (quasi)-particle spectrum in the confined phase close to  $T_c$  require a more thorough understanding, as the temperature dependence of hadron masses and other hadronic parameters will lead to observable consequences in current, and especially forthcoming, heavy ion collisions.

The temperature dependence of various hadronic properties has been addressed using a number of different approaches. These calculations yield different predictions for the behaviour of some quantities [4]. Since these approaches have limited applicability at high temperatures, one may hope that a lattice calculation of the variation with temperature of any of these quantities below the phase transition may shed light on the discrepancies.

Another important quantity is the ratio of the chromo electric to chromo magnetic screening length. This is used, for example, in estimates of the colour transparency of the plasma [5]. One promising approach is to calculate it directly from measurements of the gluon self energy on the lattice.

Recent results on the equation of state for pure gluon SU(3) theory and for QCD with two light flavours will be presented in section 2. The results from a study of hadronic properties in quenched QCD at temperatures between  $0.75T_{\rm c}$  and  $0.92T_{\rm c}$  are presented in section 3. Section 4 contains the results pertaining to the chromo electric and magnetic screening masses.

## 2 Equation of State

Recent work [6] has enabled the calculation of the energy density and pressure on the lattice using an entirely non-perturbative technique for the first time. This requires detailed a knowledge of  $dg^{-2}/da$ , ie. one needs to know the QCD beta function  $\beta_{\rm f}$  relating changes in physical quantities with changes in the coupling. This has been calculated by the TARO collaboration [7].

Given the beta function one calculates the interaction measure, the difference between the energy density and thrice the pressure, as follows:

$$\frac{\epsilon - 3p}{T^4} = T \frac{\partial}{\partial T} \left( \frac{p}{T^4} \right) = a \left( \frac{dg^{-2}}{da} \right) 6N_c N_\tau^4 \{ P_\sigma + P_\tau - 2P_0 \}. \tag{2.1}$$

The pressure is given by

$$\frac{p}{T^4} = \frac{-f}{T^4} \Big|_{\beta_0}^{\beta} = 3N_{\tau}^4 \int_{\beta_0}^{\beta} d\tilde{\beta} \left\{ P_{\sigma}(\tilde{\beta}) + P_{\tau}(\tilde{\beta}) - 2P_0(\tilde{\beta}) \right\}$$
 (2.2)

The zero temperature plaquette is given by  $P_0$ , the spatial and temporal plaquettes at finite temperature are given by  $P_{\sigma}$  and  $P_{\tau}$  respectively. Both the energy density and the pressure are normalised to zero at zero temperature.

Figure 1: The interaction measure  $(\epsilon - 3P)/T^4$  against temperature for three different values of the temporal extent  $N_{\tau}$  in pure SU(3) gauge theory.

Figure 2: The energy density compared to the energy density in the Stefan-Boltzmann limit on a lattice of the same size against the temperature in units of the critical temperature.

The results obtained for the interaction measure, divided by  $T^4$ , are shown in figure 1. The peak in the interaction measure shortly after the first order deconfinement phase transition shows clearly the strong deviation from ideal gas behaviour,  $\epsilon = 3P$ . The energy density rises sharply, whilst the pressure lags behind until one has reached temperatures around  $3T_c$ . This is evident again in figure 3 where the energy density and pressure, scaled with  $T^4$  are plotted together.

Note that the interaction measure is related to the value of the gluon condensate at finite temperature [8, 9] via

$$\langle G^2 \rangle_T = \langle 0|G^2|0\rangle - (\epsilon - 3P)_T,$$
 (2.3)

where  $\langle G^2 \rangle_T$  and  $\langle 0|G^2|0 \rangle$  are the condensates at zero and finite temperature respectively. The gluon field strength  $G^2$  is given by  $G^2 = -[\beta_{\rm f}/(2g^3)]G^{\mu\nu}_aG^a_{\mu\nu}$ . Taking  $\langle 0|G^2|0 \rangle = 0.0135 {\rm GeV}^4$  [9] one finds that  $\langle G^2 \rangle_T$  drops to zero immediately after the phase transition, and then goes negative according to the above equation.

The energy density for different values of the temporal extent is plotted in figure 2, compared to the Stefan-Boltzmann limit on this size lattice. If one takes the continuum limit one obtains a value around 83% of the Stefan-Boltzmann value for temperatures above  $2T_{\rm c}$  up to at least  $3T_{\rm c}$ . It is clear that even at these temperatures the interactions and masses of the excitations cannot be neglected. A similar rapid rise in the energy density, and slower rise in the pressure, is seen in the case of two flavour QCD [10].

It is clear that, if there is a jump in the energy density, the pressure will lag behind in a thermodynamic system, from the relation  $P/T = P_0/T + \int dT \epsilon/T^2$ .

sure in units of  $T^4$  on a lattice of size  $c_s^2 = dP/d\epsilon$  as a function of temperature  $32^3 \times 6$ . Also shown is the continuum on lattices of size  $16^3 \times 4$  and  $32^3 \times 6$  as a Stefan-Boltzmann limit (lower solid line) function of temperature. and the Stefan-Boltzmann limit for this size lattice (upper solid line).

Figure 3: The energy density and pres- Figure 4: The speed of sound squared,

The deviation from the ideal gas behaviour may be understood in terms of plasma consitituents that are massive, and have a strong interaction [11].

The speed of sound in a medium is another important parameter. This is shown in figure 4 for the high temperature phase of pure gauge theory. The speed of sound also approaches the ideal gas value  $(1/\sqrt{3})$ , but is only at around 80% of it even at  $2T_{\rm c}$ .

#### 3 **Hadronic Properties**

#### Chiral Sector 3.1

The quark condensate, the quantity from which other approaches obtain much of the effect of temperature on the hadrons, is the logical place to start. It is known to change drastically at the deconfinement transition in quenched QCD.

The chiral condensate is shown in figure 5(a) as a function of bare quark mass at  $T = 0.92T_c$ . It may be calculated directly from the trace of the fermion matrix  $(\langle \bar{\psi}\psi \rangle_{\rm SE})$  and by using the pion and sigma propagators, which corrects for the linear dependence on the quark mass [19]. One can see quite clearly that both methods extrapolate to the same value at zero quark mass. The same holds true for lower temperatures.

The temperature dependence of the chiral condensate is shown in figure 5(b), where the ratio of the finite temperature chiral condensate to that at T=0 is plotted.

Figure 5: Figure (a) shows the chiral condensate as a function of the bare quark mass, at  $\beta=6.00$ . The upper curve is obtained using the value taken directly from the trace of the fermion matrix, the lower curve after subtracting the linear dependence on the quark mass. The results have been taken from [12, 13]. Figure (b) shows the finite temperature chiral condensate normalised to its value at zero temperature. The circles represent quenched data, extrapolated to zero quark mass from [12]. The other figures represent results for various numbers of flavours, but not extrapolated to zero quark mass.

These values have been extrapolated to zero quark mass, which is the reason why the error bars are so large. If one does not extrapolate, the ratio remains the same, but with errors a factor of ten smaller. For comparison results for full QCD, including dynamical fermions, have been included. Since none of these results are at the physical quark mass, the effect of temperature is probably underestimated. It is clear that the chiral condensate does not change significantly until one is extremely close to the critical temperature.

The pion mass displays the behaviour expected of a Goldstone particle,  $m_{\pi}^2 = A_{\pi}m_{\rm q}$ , at all temperatures. There is also no sign of a dependence on temperature in the pion mass, or in the slope  $A_{\pi}$ .

Another quantity of considerable interest for understanding the temperature dependence of the chiral sector of QCD is the pion decay constant. It can be determined directly from the relevant matrix element on the lattice [19]. At zero temperature  $f_{\pi}$  is related to the chiral condensate and the pion mass through the Gell-Mann–Oakes–Renner relation, which is expected to be valid as long as chiral symmetry remains spontaneously broken.

$$m_{\pi}^2 f_{\pi}^2 = m_{\rm q} \langle \bar{\psi}\psi \rangle_{(m_{\rm q}=0)}$$
 (3.4)

The temperature independence of the amplitude,  $A_{\pi}$ , and the chiral condensate up to  $T = 0.92T_{\rm c}$  indicates that the pion decay constant will also be temperature independent. A direct calculation shows that it is, and that the GMOR relation holds, for temperatures up to at least  $T = 0.92T_{\rm c}$ .

## 3.2 Nucleon and meson masses

One obtains hadron screening masses by fitting the exponential decrease of the correlator  $C_{\rm H}(z)$  to, for example, an hyperbolic cosine. One obtains either local masses, if only two points are fitted to, or an estimate of the lowest state if one fits to the long distance part of the correlator. The lowest mass which can be extracted from the fit,  $E_{\rm H}$ , is related to the screening mass for fermionic states via

$$E_{\rm H}^2 = m_{\rm H}^2 + k \sin^2\left(\pi/N_{\tau}\right),\tag{3.5}$$

due to the contribution from the non-vanishing Matsubara energy,  $p_0 = \pi T$ . Note that for bosons  $E_{\rm H}^2 = m_{\rm H}^2$ .

The local rho screening masses and the value obtained from a fit to the full propagator at  $T=0.92T_{\rm c}$  and at zero temperature are shown in figure 6(a). It is clear that the rho screening mass does not show any significant dependence on temperature.

The nucleon has been examined using wall sources at a quark mass of 0.01 in lattice units. The local screening masses for  $T = 0.92T_c$ , and the screening mass obtained from a full fit, are shown in figure 6(b) along with the result obtained at zero temperature. The increase in temperature clearly has a dramatic effect on the nucleon. However, most of this can be understood purely in terms of the fact that the lowest momentum of the nucleon is not zero, but  $\pi T$ , as discussed above.

The screening mass at  $T = 0.92T_c$ , extracted using eqn. 3.5 with the assumption that k = 1, indicates that the mass rises slightly:  $m_{\rm n}(0.92T_{\rm c}) = (1.1\pm0.03)m_{\rm n}(T=0)$ . We note, however, that there is also the possibility of a modification of the energy dispersion relation at finite temperature, which may lead to a deviation of k from unity [20]. The error given above is from the statistical error alone, as we cannot determine the systematic error which may be introduced by our assuming that eq. 3.5 with k=1 is applicable.

Finally, one would like to know the properties of correlators with hadronic quantum numbers in the deconfined phase. These can be studied using correlators in the spatial direction, as above. One finds that the nucleon then approaches thrice the lowest Matsubara frequency, and all mesons other than the pion approach twice the lowest Mastubara frequency (see [14] and references therein). This is what one expects if the quarks become deconfined.

The pion, though, acquires a screening mass half as large as expected for a free meson. As it is the particle associated with chiral symmetry, one may expect it to have a special role even above the phase transition [22]. In order to understand whether the pion is indeed deconfined as well, with a different interaction between the two quarks, the meson correlators were examined using different techniques [23]. In one of these, temporal correlators generated with wall sources were examined. Temporal correlators show the true mass, and not the screening mass. Wall sources are used in order to project out only the contribution from the lowest state. The results for the local masses are shown in Figure 7, along with results for the effective quark mass.

One sees here that both the rho and the pion masses tend towards twice the effective quark mass at high temperatures. This, combined with other investigations

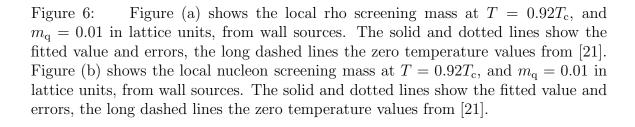


Figure 7: Local masses  $m_{\rm H}^{\rm W~(=wall)}$  from correlators constructed with wall sources in the PS (circles) and V (squares) channels in the high temperature phase. Also shown is  $2m_q^{\rm eff}$  (triangles) from [24]. Lines have been drawn to guide the eye.

on the lattice, indicate that the hadrons (including the pions) become deconfined above  $T_c$ , with rather large channel dependent residual interactions.

One does, in all cases, see the factor of two difference between the pion and rho masses or screening masses. There is clearly a difference between a quark—antiquark pair carrying pion quantum numbers and one carrying rho quantum numbers. Explanations for the relative lightness of the pion have been put forward based on spin—spin interactions [25] and residual gluon condensates [26].

## 4 Electric and Magnetic Screening Masses

The chromo electric screening mass can be obtained by examining, amongst others, the correlation between Polyakov loops or the pole of the gluon correlator. At high temperature in perturbation theory at next to leading order it has been shown that the two approaches yield the same result [27, 28].

The chromo magnetic mass cannot be determined in perturbation theory, due to infra-red divergences. Preliminary results from calculations in progress [29], in pure gauge theory, indicate that the magnetic and electric screening masses have the same order of magnitude above the phase transition, and for temperatures as high as  $2T_c$ . This result is consistent with the results obtained in another study in SU(2) pure gauge theory [30].

This can be compared with the results from the potential, and the spatial string tension [31] which indicate that the coupling remains large well above the phase transition, with  $g(T=2T_c)\approx 2$ .

## 5 Conclusions

The chiral condensate does not show any significant temperature dependence up to  $T = 0.92T_{\rm c}$ . In view of this the observation that there is no sign of a temperature dependence in the pion decay constant, pion screening mass, sigma screening mass or the rho screening mass may not come as a surprise. There is some, albeit inconclusive, indication of a temperature dependence for the screening mass of the nucleon.

The details of the temperature dependence may change in the case of QCD with two flavours, where the transition is expected to be second order rather than first order as in the the pure SU(3) gauge theory, and with quark masses close to the physical quark mass. However, these differences will probably not show up for temperatures less than  $0.9T_{\rm c}$ .

The equation of state for pure gauge theory is now reasonably well understood. One finds clear evidence for a departure from the ideal gas at below  $2T_c$ , at which point the energy density reaches only 83% of the Stefan-Boltzmann limit. Thus it is clear that there are strong interactions, or equivalently a large contribution from non-perturbative effects, above the phase transition. This is supported by measurements of the spatial string tension, which indicate a coupling  $g \approx 2$ , results for the chromo electric and magnetic screening masses, as well as the effective quark mass in the Landau gauge.

All states with hadronic quantum numbers appear to be deconfined above the phase transition. However, the coupling between the quark and anti-quark depends on the channel considered, leading to pion / sigma masses of around half the rho mass.

## Acknowledgements

The results discussed here have been supported in part by the Stabsabteilung Internationale Beziehungen, Kernforschungszentrum Karlsruhe, a NATO research grant, contract number CRG 940451 and a DFG grant, DFG Pe-340/1, DFG Pe-340/6-1, and the HLRZ in Jülich. I would like to thank the organisers of the conference for the invitation and the support received. I would also like to thank my colleagues, J. Engels, S. Gupta, F. Karsch, E. Laermann, C. Legeland, M. Lütgemeier, B. Petersson and K. Redlich for enlightening discussions and productive collaboration.

# References

- [1] I. Montvay and G. Münster, *Quantum Fields on the Lattice*, Cambridge Monographs on Mathematical Physics, Cambridge University Press, Cambridge, 1994.
- [2] F. Karsch, in *Quark-Gluon Plasma*, R. Hwa, ed., vol. 6 of Advanced Series on Directions in High Energy Physics, World Scientific, 1990.
- [3] B. Petersson, Nucl. Phys. B [Proc. Suppl.] 30 (1992) 66. F. Karsch, Nucl. Phys. B [Proc. Suppl.] 34 (1993) 63. C. DeTar, hep-lat 9412010, Nucl. Phys. B [Proc. Suppl.] (1995), to be published. K. Kanaya, hep-lat 9502020, UTHEP-296.
- [4] H. Leutwyler and A. V. Smilga, Nucl. Phys. B 342 (1990) 302. G. E. Brown and M. Rho, Phys. Rev. Lett. 66 (1991) 2720. T. Hatsuda, Y. Koike, and S. H. Lee, Nucl. Phys. B394 (1993) . C. Adami and G. E. Brown, Phys. Rep. 234 (1993) 1. C. A. Dominguez and M. Loewe, preprint UCT-TP-208-94, 1994. V. L. Eletsky and B. L. Ioffe, Phys. Rev. D47 (1993) 3083.
- [5] M. Gyulassy and A. V. Selikhov, in *Quark Matter '93*, Nucl. Phys. A566 [Proc. Suppl.], 1994.
- [6] J. Engels, Phys. Lett. B 252 (1990) 625. J. Engels, F. Karsch, and K. Redlich, Nucl. Phys. B 435 (1995) 295
- [7] K. Akemi et al., Phys. Rev. Lett. **71** (1993) 3063.
- [8] D. E. Miller, preprint BI-TP 94/41, Bielefeld, 1994.
- [9] H. Leutwyler, in *QCD 20 years later*, P. M. Zerwas and H. A. Kastrup, eds., World Scientific.
- [10] T. Blum et al., preprint IUHET-284, 1984.

- [11] D. H. Rischke et al., Phys. Lett. B **278** (1992) 19-23.
- [12] G. Boyd et al., Phys. Lett. B, to be published; BI-TP 94/42, hep-lat 9501029.
- [13] R. Gupta et al., Phys. Rev. D 43 (1991) 2003.
- [14] R. V. Gavai et al., Phys. Lett. B **241** (1990) 567.
- [15] R. Altmeyer et al., Nucl. Phys. **B389** (1993) 445.
- [16] J. Kogut and D. K. Sinclair, Phys. Rev. Lett. 60 (1988) 1250. Nucl. Phys. B 344 (1990) 238.
- [17] J. Kogut, D. K. Sinclair, and K. C. Wang, Phys. Lett. **B 263** (1991) 101.
- [18] F. Karsch and E. Laermann, Phys. Rev. **D** 50 (1994) 6954.
- [19] G. Kilcup and S. R. Sharpe, Nucl. Phys. **B283** (1987) 493.
- [20] D. Lissauer and E. V. Shuryak, Phys. Lett. **B 253** (1991) 15.
- [21] S. Kim and D. K. Sinclair, Nucl. Phys. B [Proc. Suppl.] **34** (1993) 347.
- [22] T. Hatsuda and T. Kunihiro, Phys. Rev. Lett. **55** (1985) 158.
- [23] G. Boyd, S. Gupta, F. Karsch, and E. Laermann, Z. für Phys. C 64 (1994) 331.
- [24] G. Boyd, S. Gupta, and F. Karsch, Nucl. Phys. B 385 (1992) 481.
- [25] V. Koch et al., Phys. Rev. D 47 (1992) 2157.
- [26] M. Ishii and T. Hatsuda, Phys. Lett. **B** 338 (1994) 319.
- [27] A. K. Rebhan, Nucl. Phys. **B 340** (1994) 319.
- [28] E. Braaten and A. Nieto, Phys. Rev. Lett. **73** (1994) 2402.
- [29] Bielefeld Quadrics Group, Work in Progress.
- [30] U. Heller, F. Karsch, and J. Rank: Work in Progress.
- [31] E. Laermann et al., Nucl. Phys. B [Proc. Suppl.] to be published (1995).